(Preprint) AAS 25-XXXX

TIME SENSITIVE DEPARTURES IN NEAR RECTILINEAR HALO ORBITS

Marielle M. Pellegrino[*], Cesar Ocampo [†], and Christopher Foster [‡]

Satellites in a Near Rectilinear Halo Orbit can utilize unstable manifolds for departure to heliocentric orbits at their end of life. These orbits are highly sensitive to dispersions due to navigation uncertainties and maneuver execution errors. Additionally, uncertainties due to orientation can cause varying effects of solar radiation pressure and out-gassing events can occur after a satellite is no longer operational. This paper characterizes how operators can minimize time of contact with their satellites post-departure while avoiding collisions with other celestial bodies and spacecraft in the orbit used by Earth-Moon's 9:2 NRHO resonance.

1 INTRODUCTION

The Near Rectilinear Halo Orbit (NRHO) the Gateway will be using constitutes the primary feature the Artemis Program's cislunar space infrastructure is built around[1] . Artemis III and subsequent missions will be utilizing this eclipse-avoiding 9:2 resonant orbit for lunar access.[2] The NRHO is considered a staging orbit for human travel beyond lunar orbit.[3] Beyond human exploration, the NRHO has unique dynamical properties, which make it useful for other programs. The NRHO has been considered a possible stopping point for near-Earth asteroid missions with an additional focus on asteroid mining.[4] Ensuring the NRHO has a long lifetime for orbital use involves taking into account orbital debris issues before they arise. Preserving the orbit involves protecting it from the risk of collisions with lingering debris to make it safe for operational use.[5] This is critical for humanity's sustained presence at the Moon and beyond. Therefore, it is important that we develop best practices for disposing of satellites after their active lifetimes while taking into account operational constraints individual entities may have.

There exist multiple solutions for protecting orbits from debris for sustained use. Graveyard orbits have offered possible solutions for orbits beyond low Earth where it is expensive to do a reentry maneuver and Earth's atmosphere is no longer naturally decaying the altitude of the orbits. Geosynchronous (GEO) orbit has a mandated graveyard orbit for satellites at their end of life. However, many satellites don't have the fuel left at their end of life to reach these orbits.[6] A greater potential issue for using this approach for satellites in the NRHO is that highly unstable environments like those close to the NRHO are too risky for graveyard orbits. At medium Earth orbit which is subject to nearby destabilizing resonances from the Sun and Moon, Pellegrino et al. found that graveyard orbits aren't as feasible due to debris interacting with nearby orbits.[7] The NRHO and cislunar environment have been studied for debris cloud evolution where nearby unstable manifolds can result

[*]Astrodynamics Engineer, Odyssey Space Research, LLC, 1120 NASA Pkwy, Suite 505, Houston TX, 77058
[†]Deceased, Astrodynamics Engineer, Odyssey Space Research, LLC, 1120 NASA Pkwy, Suite 505, Houston TX, 77058
[‡]Aerospace Engineer, Flight Mechanics and Trajectory Design Branch, NASA, Johnson Space Center, Houston, TX 77058

in unplanned impacts to the surface of the Moon.[8–10] Boone et al. showed that after a year, twenty percent of the debris cloud originating from the NRHO impacted the moon.[11]

Instead of working against the local instabilities close to the NRHO, this paper utilizes them as a means of disposal. Breakwell et al. first defined the type of Halo orbits originating from the Earth-Moon L1 and L2 locations which built the foundation of this methodology.[12] Leveraging unstable manifolds as a means to access different orbital regimes has been long studied. Howell et al. used unstable manifolds to develop trajectory arcs for access to libration points.[13] Koon et al. used heteroclinic connections for transfers between L1 and L2 periodic orbits.[14]

More recently there has been extensive analysis on exploiting three body dynamics for departures from the NRHO with the purpose of disposal of objects in Gateway's vicinity.[15–17] Davis et al. have studied the possible collision risks disposed objects can post to the Gateway after their departure from the NRHO.[18]

Scheuerle et al. showed that maximizing angular momentum out of the Earth-Moon plane will maximize the Sun-Earth energy, essentially ensuring a highly energetic departure through the L1 and L2 portals.[19] Davis et al. demonstrated that heliocentric orbits can be characterized 600 days out from jettison. This inference helps understand how far upstream one needs to target the heliocentric orbit without the sensitivities of Sun-Earth geometry affecting the behavior each epoch.[20] Their work has focused on clean-up maneuvers occurring at the two-week mark. This investigation builds upon previous disposal characterization findings and focuses on adding to the departure catalog by determining the shortest time of contact needed for clean-up maneuvers.

The methods used in this paper for targeting departure from the Earth-Moon System to heliocentric space are in accordance with those used by previous researchers in which a statistical approach by means of the Monte Carlo simulations is exploited. Orbital uncertainties due to navigation and maneuver execution are modeled and incorporated in the study to guarantee higher fidelity and understanding of the rapid departure cases. The results are then compared and validated against previous studies.

2 METHODOLOGY

2.1 Finding the Optimal Departure

The trajectories presented in this study are converged and propagated using Copernicus, NASA Johnson Space Center's trajectory design and optimization software, with SNOPT.[21] The departure trajectories are built with a direct multiple shooting point method. To avoid the highly dynamic region near perilune, we constrain departure to occur no closer than a half day before perilune. The exact location on the NRHO for departure is chosen by the optimizer and is allowed to vary between apolune and the perilune constraint.

The timing of all the flybys are also chosen by the optimizer; each flyby is set as a node for the multiple point shooting method. This is done by describing the state in terms of orbital elements at the node location and setting every value as an optimization variable except true anomaly; the radius of periapsis is also forced to be over 100km altitude to prevent the optimizer from choosing trajectories that come close to the Moon.

Following the flybys, a node is placed at the corner turn where the trajectory is departing the moon. The location of this node is set to be 45000km from the Earth through a magnitude of the position vector constraint. To achieve a departure from the Moon, we maximize the angular

momentum out of the Earth-Moon orbital plane at this location. The optimizer is solved at this stage to ensure a trajectory that is departing the Moon and heading toward either L1 or L2 point. This sets up the optimzier with good initial conditions to target its final disposal orbit.

Once the vehicle departs the Moon, the way points are set to axis crossings of the Earth-Sun system and eventually through the L1 or L2 portals to the final heliocentric state 600 days from the departure time. We use the previous solved departure from the lunar vicinity as an initial guess for targeting a final heliocentric orbit. This heliocentric orbit is chosen to have with a period and argument of perihelion such that the vehicle will minimally interact with the Earth-Moon System. This is done by setting the timing such that during periods where the vehicle laps the Earth-Moon system it is at perihelion and the Earth is at aphelion. In the case of the exterior orbit, the vehicle is lapped while at aphelion and the Earth is at perihelion. In either case, the ideal placement is when the orbits lap each other, the interior one is at perihelion and the exterior one is at aphelion to ensure maximum distance and no energy transfer from the flyby while on the 50 year trajectory. Energy transfer from a flyby is the quickest way for dispersions to grow in the data and for trajectories to be caught by the Earth-Moon system.

2.2 Dispersion Modeling

To model operational dispersions, the truth state of each Monte Carlo run and the burn solver's dispersed state are separately tracked. The Monte Carlo is first initialized with dispersion about the reference NRHO kernel.[22] This state is then dispersed by the navigation uncertainties and that value is sent to a separate file to solve the burn. After the burn is solved, the delta v value is dispersed by the maneuver execution errors and sent to the truth ideck to be implemented and propagated forward. The subsequent trajectory correction maneuvers are calculated in the same fashion. Figure 1 shows a visualization for how the initial and navigation dispersions are sampled and sent to the burn solving routine.

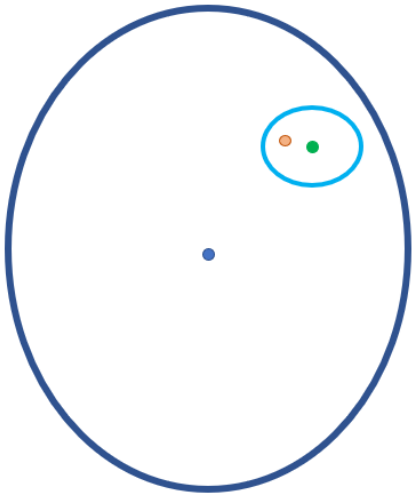

Figure 1: Dark blue circle represents the initial dispersions. Green represents the truth state sampled in the initial dispersion set. The light blue represents the navigation dispersions and the orange dot represents the estimated state sampled and sent to the solver.

For each Monte Carlo run, the exit and subsequent trajectory correction maneuvers are calculated in Copernicus. After the final trajectory correction maneuver, the trajectories are propagated to their departure of the Earth-Moon system and then solved for outside of the Copernicus software. This allows for proper switching of dynamical models between orbital regimes for Monte Carlo cases where the object does reenter the Earth-Moon system. A model of the logic of how the states are separately tracked and eventually sent to the final propagation is shown in Figure 2. The gravitational accelerations are still modeled by Copernicus using its application

programming interface (API) but the integration is handled by a 7/8 order Runge-Kutta integrator in Python. Although the propagation is long, fifty years, the disposed satellite spends majority of its time in heliocentric orbit where the integrator can take larger steps which leads to less error accumulation over that time period. For this study, the number of steps the integrator takes is tracked to ensure no large creep in error due to uncertainty of propagation influencing the result. In the case where the vehicle reenters the Earth-Moon system and stays, we make mention of the possible degradation of performance of the simulation for that case.

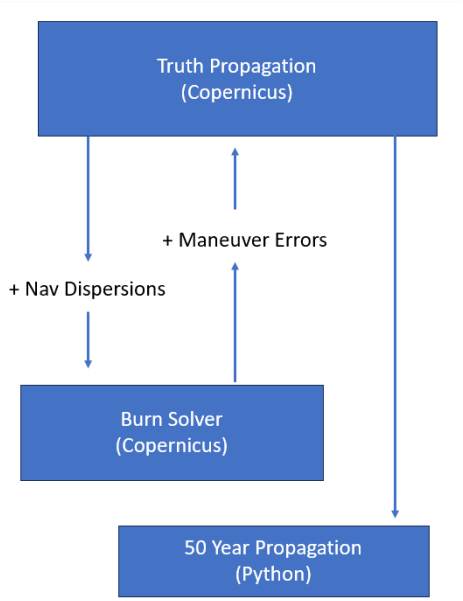

Figure 2: Chart of the algorithm logic in how the truth state of the vehicle is separated in Copernicus and eventually is sent to Python for the final propagation.

3 EARTH-MOON GEOMETRY

The geometry of the Earth-Moon system is increasingly important in the case of rapid departures. Because there are only two ways to depart, either to an interior heliocentric orbit through the Earth-Sun L1 portal or to an exterior heliocentric orbit through the Earth-Sun L2 portal, there are two ideal times to leave the NRHO to get through these portals. A satellite can depart on any revolution of the NRHO and achieve a heliocentric departure but to do so in the least amount of time constrains the problem to specific locations. This is due to the timing of the departure. For lower energy departures that spend many flybys before departing, there is more room for variation in the orientation of departure trajectory as the larger amount of time to depart is not as sensitive to the exact location in which the departure is initiated. On the other hand, a higher energy departure of about 5 or 10 m/s where the vehicle is rapidly departing the Earth-Moon system, the vehicle is departing within the first month and is constrained by where the departure is initiated. The vehicle will have a minimum of two lunar flybys before developing the velocity needed to depart and eventually make its way out of the L1 or L2 portal. Figure 3 shows the Earth-Moon geometry in a Sun-Earth frame. For an example high energy case departing to an L2 orbit, to gain enough energy through two lunar flybys to depart safely and not return the ideal location for departure is location D on Figure 3. At the next location, E, by the time the vehicle departs, it only has two flybys (since the sequence is 9:2,

possible flybys are every other location) before it needs to leave the Moon's orbit and start heading toward the L2 gateway.

Because the location of the departure burn in the Earth-Sun frame is so consequential, this paper will examine the least optimal locations to depart the Earth-Moon system. This will help determine the edge case of how great an influence requiring an additional flyby due to the timing of leaving through the L1 and L2 portals will affect the time needed to remain in contact with the vehicle.

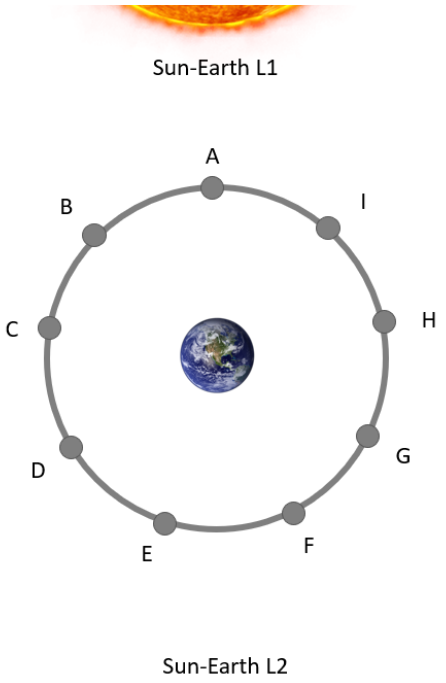

Figure 3: Visualization of NRHO perilune locations with respect to the Earth in a Sun-Earth frame. Each letter and dot corresponds with a revolution of the NRHO. The letters do not signify sequential order as the Moon orbits the Earth twice for the full 9 revolution of the NRHO.

4 BASELINE DEPARTURES

The idealized departures from the Moon will be sectioned by the Earth-Moon geometry discussed in the previous section. Each of the nine locations has a unique timeline on how to depart the Earth-Moon system and thus a family of associated trajectories. Because time of contact is the main constraint studied, the trajectories are designed to depart the Earth-Moon system as quickly as possible.

We will focus on three cases for the departure locations. The first is location D where the geometry is ideal for an exit, having just enough time to conduct two flybys and depart through the L2 portal energetically (there exists a similar location on the opposite side for an L1 interior exit). The second is location C, one geometrical location earlier where the vehicle has to remain in the Earth vicinity for a half revolution longer than case D. The final case studied is location E where the vehicle will have to remain in the Earth vicinity the longest because it missed the last opportunity to depart energetically with two flybys.

4.1 Location D

We will start with location D as that is ideally aligned for enough lunar flybys to depart with a 10m/s disposal burn. The case discussed is an NRHO departure two days before perilune, followed by two lunar flybys (after the departure perilune) and a corner turn departure from the Moon 27 days later. The vehicle leaves Earth's vicinity at the 42 day mark and has a final period of 394 days. This is an exterior orbit disposal that exits through the L2 Portal. The final period was chosen to be consistent with previous findings of idealized disposal targets by Davis et al.[20] The full orbital description chosen to target (most notably the argument of perihelion) was chosen to minimize close approaches to the Earth-Sun system. Figure 4 shows a Copernicus graphic of the departure.

Figure 4c shows the propagation of the nominal departure for fifty years where there are no close approaches.

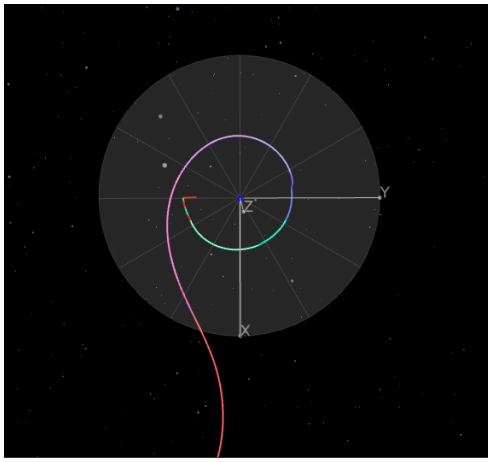

(a) Z-axis view

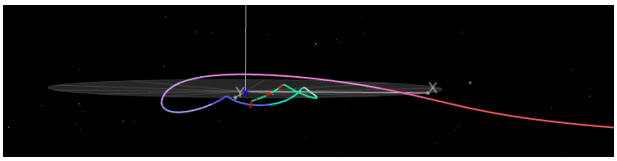

(b) Y-axis view

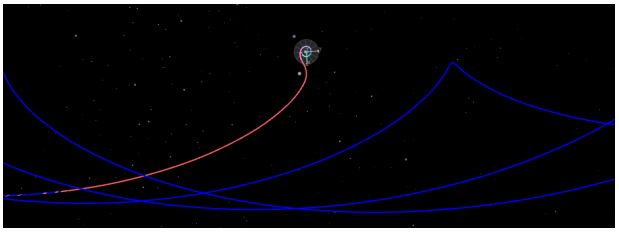

(c) Nominal 50 year trajectory in blue.

Figure 4: Copernicus graphic of the baseline disposal trajectory from perilune location D. The graphic is in a Sun-Earth rotating frame centered at the Earth (x-axis is pointing away from the Sun).

4.2 Location E

At perilune location E the vehicle no longer has time to gain enough energy for a rapid exit out the L2 portal. Therefore, the next opportunity to leave the Earth system is through the L1 portal to an interior disposal orbit a half a lunar orbit later. For this trajectory, the vehicle departs the NRHO one day before perilune. It then has three lunar flybys before reaching the corner turn exit from the Moon 40 days later. Then the vehicle leaves the Earth's vicinity at the 50 day mark for an exit to an interior orbit. The final orbital period is 338 days. This exit is shown in Figure 5. The interior final orbit avoids close approaches of the Earth-Moon system over the fifty years.

4.3 Location C

A revolution location earlier than the idealized departure, the vehicle can still exit through the L2 portal. Because this is geometrically a revolution earlier (not exactly one period earlier in the NRHO timeline), the timing to depart the Earth system is only about three days longer than location D. Thus, there isn't an additional flyby in this case; the vehicle will exit the lunar vicinity with two flybys. The baseline case for location C departs the NRHO about 0.8 days prior to perilune. Then after the two flybys, the vehicle leaves the Moon at 25 days and leaves the Earth at around 40 days to an exterior orbital period of 394 days. The trajectory is shown in Figure 6.

5 INCORPORATING DISPERSIONS

With the Sun-Earth-Moon geometries solved for their ideal departures, we will now examine how sensitive these departures are to time of contact. The time of contact will be measured from the time of the disposal burn until the time of the final trajectory correction maneuver (TCM). For times of contact studied five days or less there will be only one TCM. For time of contact longer than five

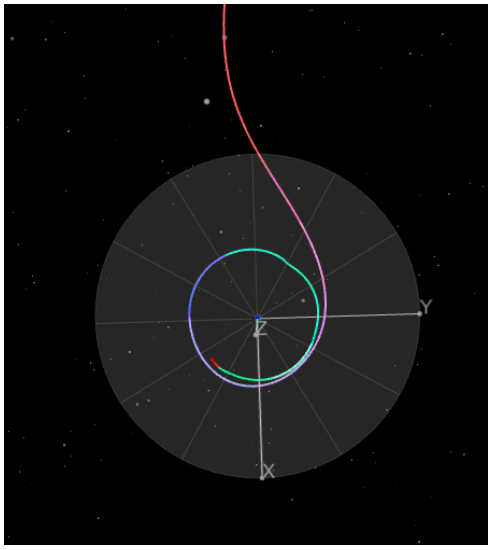

(a) Z-axis view

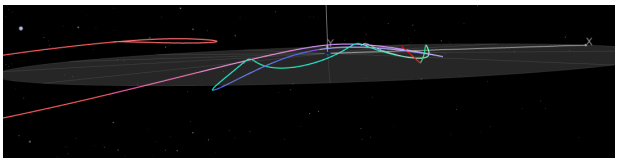

(b) Y-axis view

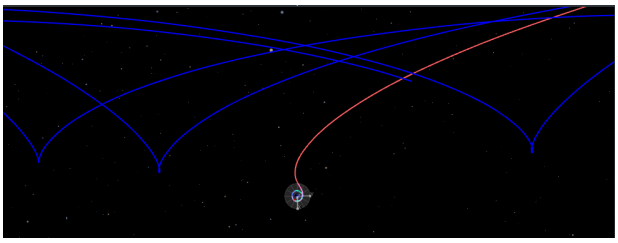

(c) Nominal 50 year trajectory in blue.

Figure 5: Copernicus graphic of the baseline disposal trajectory from perilune location E. The trajectory is in a Sun-Earth rotating frame centered at the Earth (x-axis is pointing away from the Sun).

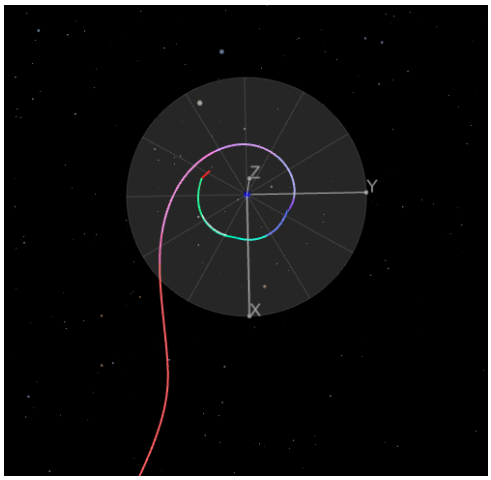

(a) Z-axis view

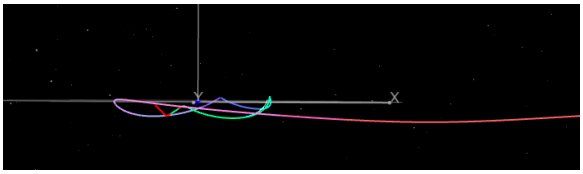

(b) Y-axis view

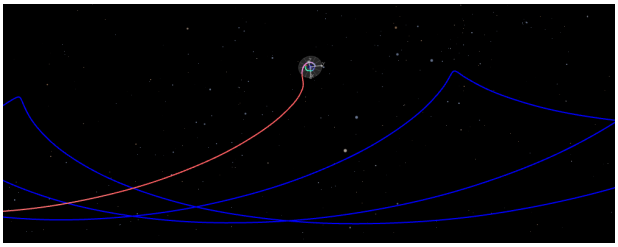

(c) Nominal 50 year trajectory in blue.

Figure 6: Copernicus graphic of the baseline disposal trajectory from perilune location C. The trajectory is in a Sun-Earth rotating frame centered at the Sun (x-axis is pointing away from the Sun).

days there will be two trajectory maneuvers, one at the five day mark and the second at the final time of contact day. Placing the TCM at the five day mark ensures that even for the longer times of contact there is a TCM to help curb dispersion post perilune pass after the disposal burn. The initial trajectory correction maneuver for those longer arcs prevents the vehicle from wandering too far and being unrecoverable depending on the dispersion. An example of the TCM placement is shown

in Figure 7. The values for the dispersions are in Table 1 and are similar to the ones Davis et al.[20]

Table 1: Dispersion Amounts

Dispersion	3σ	Unit
initial position (per axis)	3	km
initial velocity (per axis)	3	cm/s
navigation position (per axis)	10	km
navigation velocity (per axis)	10	cm/s
TCM navigation position (per axis)	1	km
TCM navigation velocity (per axis)	1	cm/s
Burn Execution Magnitude	1.5	percent
Burn Execution Pointing	1	degree
Burn Execution Bias	0.142	cm/s

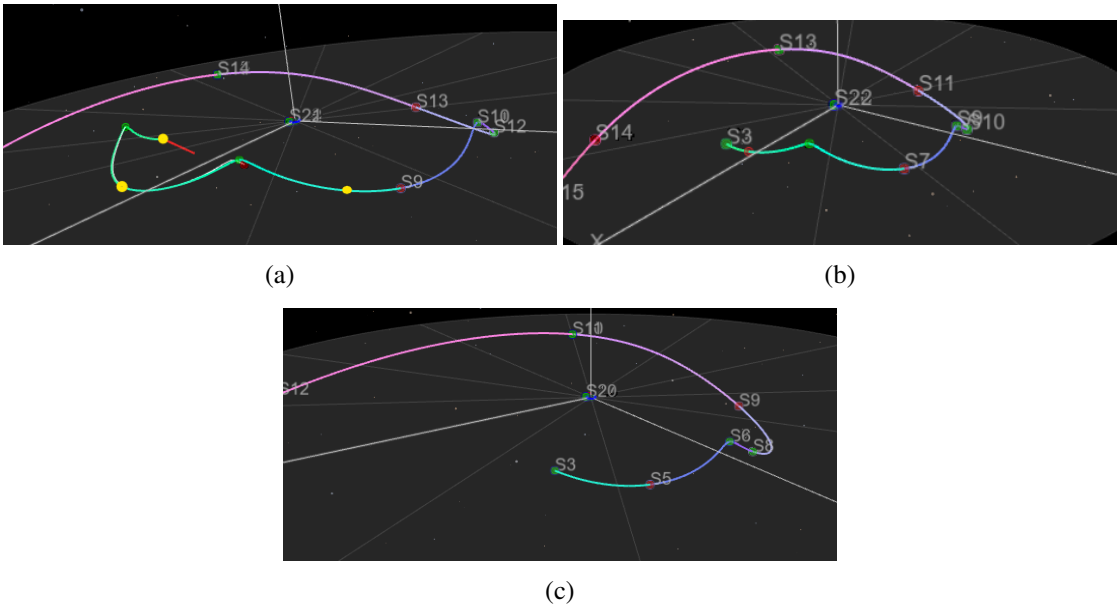

(a) (b)

(c)

Figure 7: Copernicus graphic of TCM placement. (a) Initial exit trajectory with yellow dots projected where TCMs would occur for a 10-day time of contact on an exit from Location D. (b) TCM 1 trajectory (c) TCM 2 trajectory (if applicable)

5.1 Location D

The first dispersion set is for exit for revolution location D. Because this is the ideal location of the nine to leave through L2, we find that the dispersed points generally follow the nominal exit trajectory for TCMs placed at 6-10 days. Figure 8 shows the Copernicus graphic of the departures of the 1000 Monte Carlo runs from the Earth-Moon system. The graphic segment shown here starts when the segment reaches the Earth's sphere of influence and is propagated for fifty days to illustrate the uniformity (or lack of) of the trajectories in the Monte Carlo set early in the fifty year propagation.

A final TCM at the three day mark results in trajectories that start to deviate significantly from the nominal in the early portion of the propagation. Then there is a substantial increase in the dispersion for the two day TCM location. Some of these trajectories don't even exit at the sphere of influence

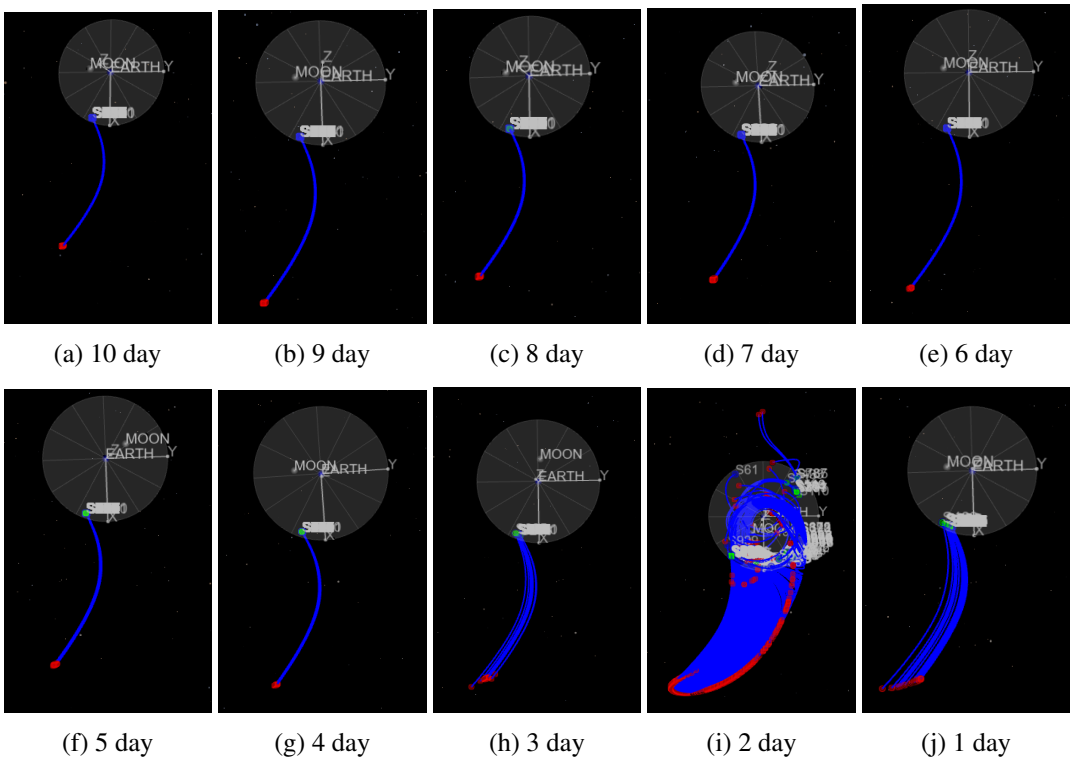

(a) 10 day (b) 9 day (c) 8 day (d) 7 day (e) 6 day

(f) 5 day (g) 4 day (h) 3 day (i) 2 day (j) 1 day

Figure 8: Copernicus graphic of the exit from the Earth's sphere of influence (for trajectories that exit) for location D. The frame is a Sun-Earth rotating frame with the Sun at the top of the page. Each subfigure shows how the departures evolve as the final TCM day changes. The day subcaption is the day of the final TCM for the set.

condition; they return at that point and continue to orbit the Earth. We see a couple cases where the trajectories exit in the opposite direction, an interior heliocentric disposal through the L1 portal instead of exterior through L2. The behavior improves for the one day TCM case.

The reason the two day case has worse performance is a result of the timing of the nominal departure. Because we discretized the space by time of contact, there will be times where the satellite is performing a trajectory correction maneuver close to perilune. This is not an ideal location on the orbit to perform a TCM because the sensitivities to navigation uncertainty and maneuver execution errors will result in larger dispersions in the data set. The two day TCM case visually shows how those sensitivities impact the overall performance of the final TCM. For reference, the Monte Carlo runs where no TCM is applied is shown in Figure 9a.

5.2 Location E

At location E the trajectory has three flybys until it departs through L1 to an interior heliocentric orbit. Because the trajectory spends more time around the Moon before departing the Earth-Moon system, we expect to see the Monte Carlo set to have greater dispersion for similar TCM times as Location D. Figure 10 shows the exits from the Earth's sphere of influence and Figure 9b shows the dispersions with no TCMs. The straight horizontal lines are indicative of an early impact with a celestial body before the trajectory was sent to the python script for the fifty year propagation. They are not actual trajectory paths.

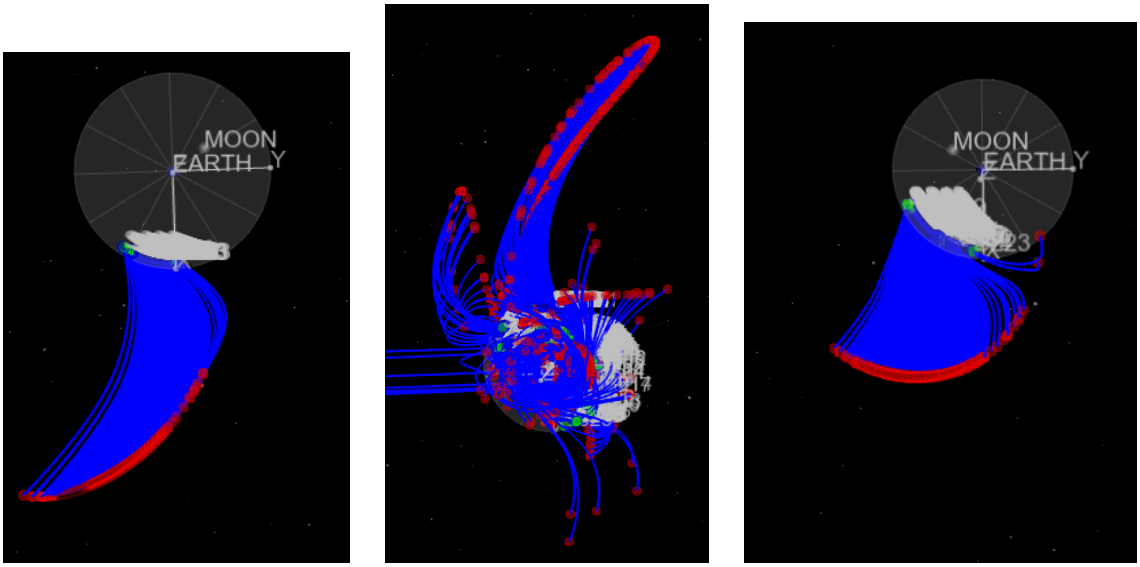

(a) Location D (b) Location E (c) Location C

Figure 9: Dispersions post disposal burn with no trajectory correction maneuver

As the day the TCM departs decreases, the dispersions of the departures increase with the exception of a TCM at eight days. This discrepancy is due to the same phenomenon seen in the two day case for location D. The eight day placement is near a flyby perilune and thus the performance of the TCM is impacted. The eight day TCM shows how these sensitivities can inhibit the performance of the TCM because there is more variety of the outbound trajectories than there is in either the six day or seven day case. However, the general trends show that as the days decrease from the last TCM, the departure trajectories start to have a larger spread.

5.3 Location C

Similar to location D, the departure from location C results in a wider dispersed set at the Earth's sphere of influence departure point, shown in Figure 11. We see a slight increase in dispersion at the eight day TCM mark consistent with the flyby time. This trajectory isn't as sensitive as the other as its departure relative to the first perilune is not as aligned in days as the original two, leaving closer to 0.8 days prior to that perilune than a day. However, the most substantial increase in dispersions occurs at the six day final TCM set. We are not certain why this behavior is seen but what could possibly be happening is at that timing there is a local solution that the solver is reaching that is much more unstable than the original disposal model. Although those types of neighboring unstable sets are more likely to occur at perilune, they can be seen at other points of the trajectory. The targeter is trying to hit the same departure period but could require additional constraints to ensure the trajectory is on a desired departure.

The dispersions tend to grow in a more logical fashion after the six-day set; decreasing the time of contact of the vehicle results in an increased dispersion on the exit. The one-day TCM case has the largest set of dispersions of them all.

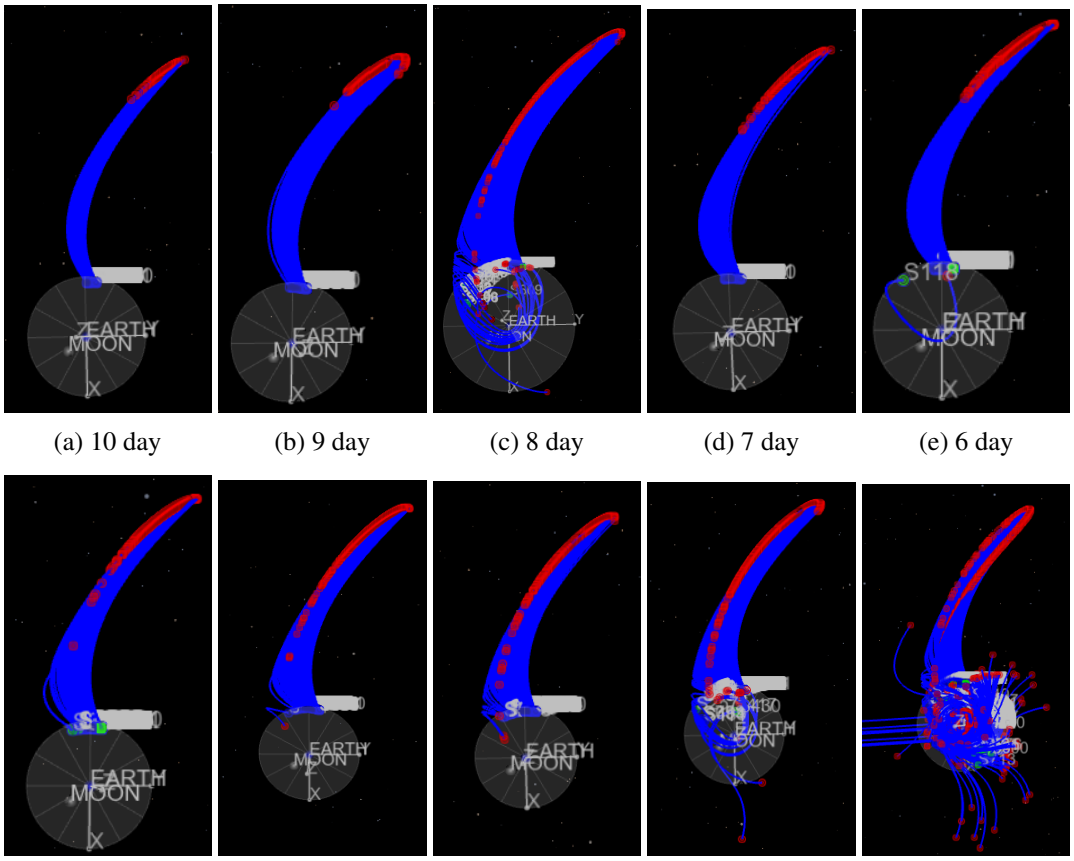

(a) 10 day (b) 9 day (c) 8 day (d) 7 day (e) 6 day

(f) 5 day (g) 4 day (h) 3 day (i) 2 day (j) 1 day

Figure 10: Copernicus graphic of the exit from the Earth's sphere of influence (for trajectories that exit) for location E. The frame is a Sun-Earth rotating frame with the Sun at the top of the page. Each subfigure shows how the departures evolve as the final TCM day changes. The day subcaption is the day of the final TCM for the set.

5.4 Earth-Moon System Interactions

These disposal trajectories were chosen so that they could not impact a planetary body, mainly the Earth or the Moon. Therefore, the Monte Carlo sets were analyzed for interactions with the Earth-Moon system. The main three thresholds for interaction are: coming back to the Earth's sphere of influence, coming below Geosynchrnous Orbit (GEO), and actual impacts on the planetary body. Although we are mainly concerned about impacts to the Earth or Moon, the other thresholds help provide additional context for the overall understanding of the statistical likelihood a trajectory will return. Example trajectories depicting a lunar impact, a flyby within GEO, and an Earth's sphere of influence entry are shown in Figure 12.

Figure 13, Figure 14, Figure 15 show these statistics as a function of the timing of the final TCM. The solutions where the TCM placement is close to perilune can confuse the overall trends, so although they are still plotted on the figure they are not incorporated in the trend lines. These trend lines are solved as third degree polynomials.

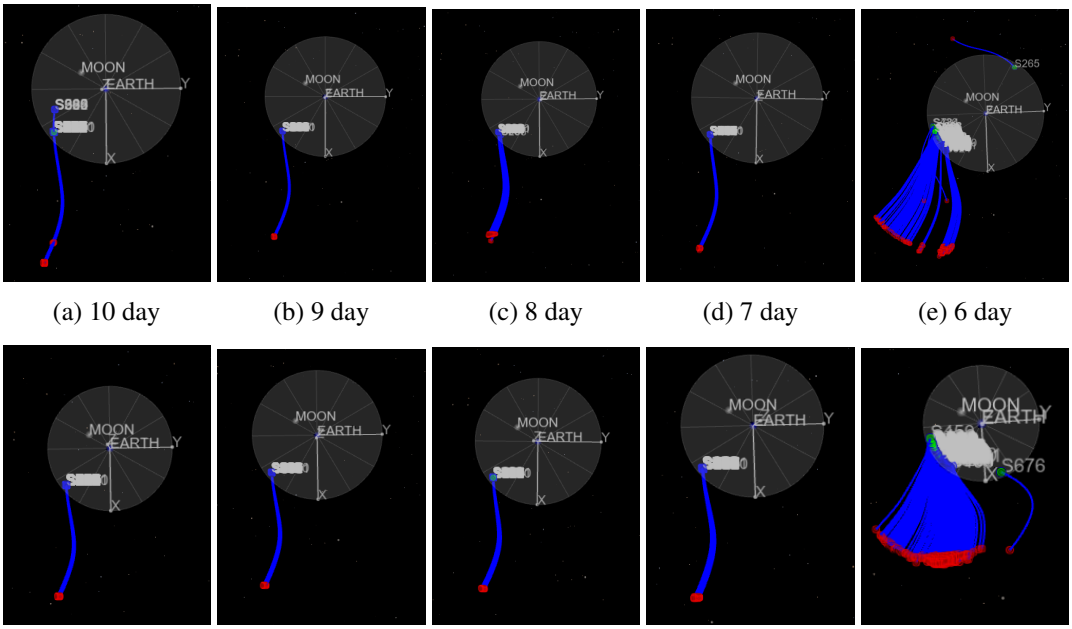

(a) 10 day (b) 9 day (c) 8 day (d) 7 day (e) 6 day

(f) 5 day (g) 4 day (h) 3 day (i) 2 day (j) 1 day

Figure 11: Copernicus graphic of the exit from the Earth's sphere of influence (for trajectories that exit) for location C. The frame is a Sun-Earth rotating frame with the Sun at the top of the page. Each subfigure shows how the departures evolve as the final TCM day changes. The day subcaption is the day of the final TCM for the set.

Overall, location E has the largest number of reentries for each set, followed by location C, and finally the location with the smallest number of reentries is location D. This follows the general theory that the longer the trajectory has to exit the Earth-Moon system, the more likely the neighboring space around that trajectory has trajectories that return to Earth. When just looking at the planetary impacts section, location E is quicker to control these dispersions with similar trajectory correction maneuver times than location C. This is part of the reason the added context of the GEO condition and Earth's sphere of influence are useful. Although location E might not have as many impacts, it does have similar amount of trajectories getting close to the Earth in its propagation.

5.4.1 Location D Predominantly, the later trajectory correction maneuvers result in less trajectories that come back into the Earth-Moon system and impact the Moon or Earth. After TCMs of about six days there are no planetary impacts for the set. For a bigger picture, no trajectories come within GEO for TCMs six days or less; at around the four day TCM Monte Carlo set, the amount of trajectories that come into GEO increases to about twenty which is close to the maximum of twenty three for no TCMs.

5.4.2 Location E The amount of times these trajectories interact with the Earth-Moon system is much larger than location D. A large amount of trajectories never leave. On the low end, at the ten day TCM location, thirty six trajectories come back to the Earth's sphere of influence and on the high end, at the one day final TCM location more than half the Monte Carlo set returns to the Earth-Moon system, 682 trajectories.

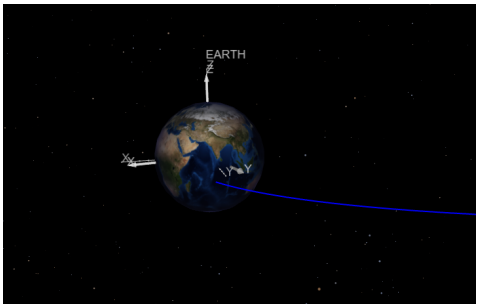

(a) Impacting Earth

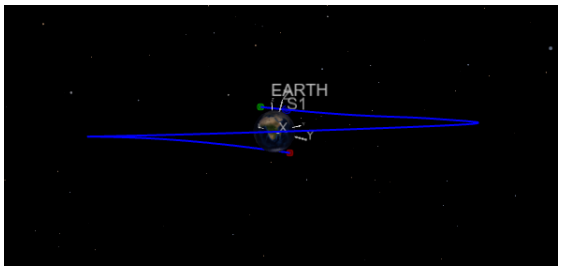

(b) Close approach within GEO (Earth view)

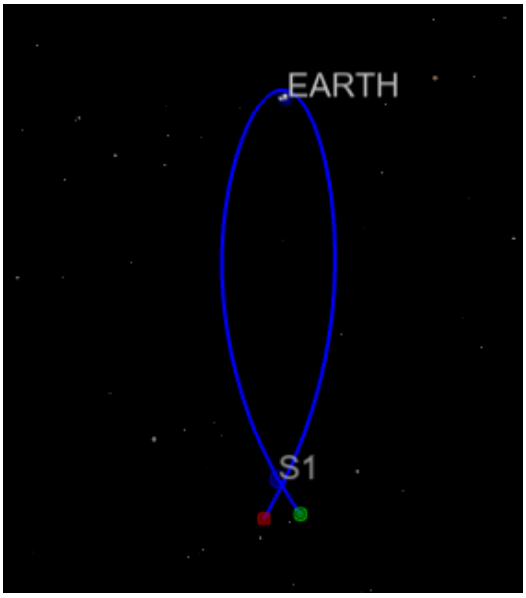

(c) Close approach - within GEO (heliocentric view)

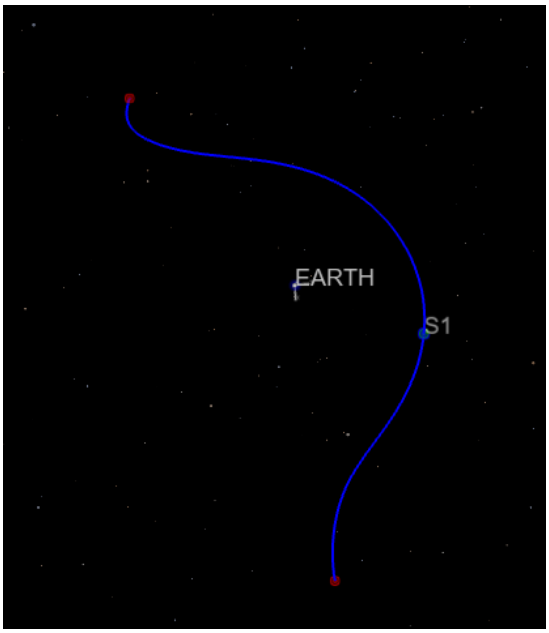

(d) Earth close approach

Figure 12: Copernicus graphics of example trajectories of interactions with the Earth. The trajectories are only plotted within the Earth's sphere of influence. The trajectory starts at the green dot (entry to the sphere of influence) and end at the red dot (departure of the sphere of influence). The graphics far from Earth are in an Earth-Sun rotating frame with the Sun at the top of the page.

5.4.3 Location C Similar to the other locations, mostly having the final TCM later in the disposal's life will result in more robust exits and non-returns. These cases drop their interactions with the Earth-Moon system at the four day TCM mark. We see the exception in this data set with how poorly the six-day TCM controls the behavior of the trajectory; the high amount of times the trajectories reenter the Earth's sphere of influence and come below the orbit of GEO. However, these trajectories don't necessarily amount to planetary impacts.

6 INTEGRATOR CONSIDERATIONS

Because the bulk of the fifty year propagation (or less time for Monte Carlo runs that impact a celestial body) is spent in heliocentric orbit where the trajectory is completing one orbit every year, the number of integrator steps the integrator took did not climb for most Monte Carlo runs.

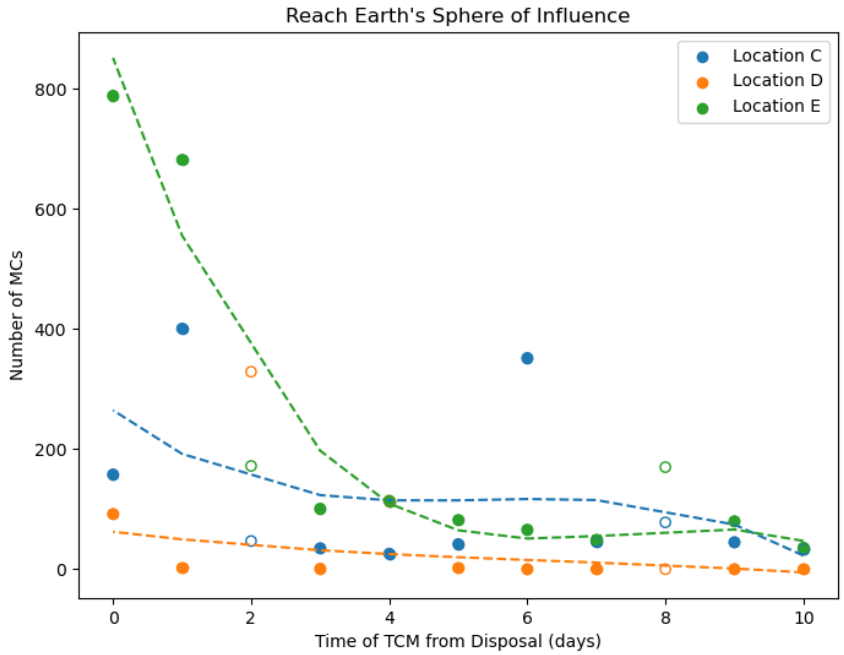

Figure 13: Number of monte carlo runs with interactions with Earth's sphere of influence

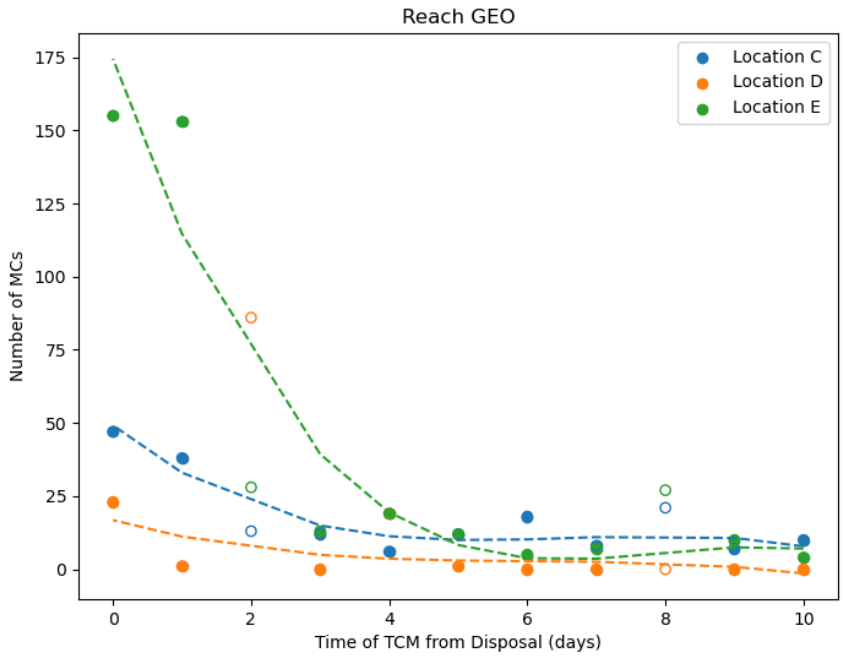

Figure 14: Number of monte carlo runs that come below GEO

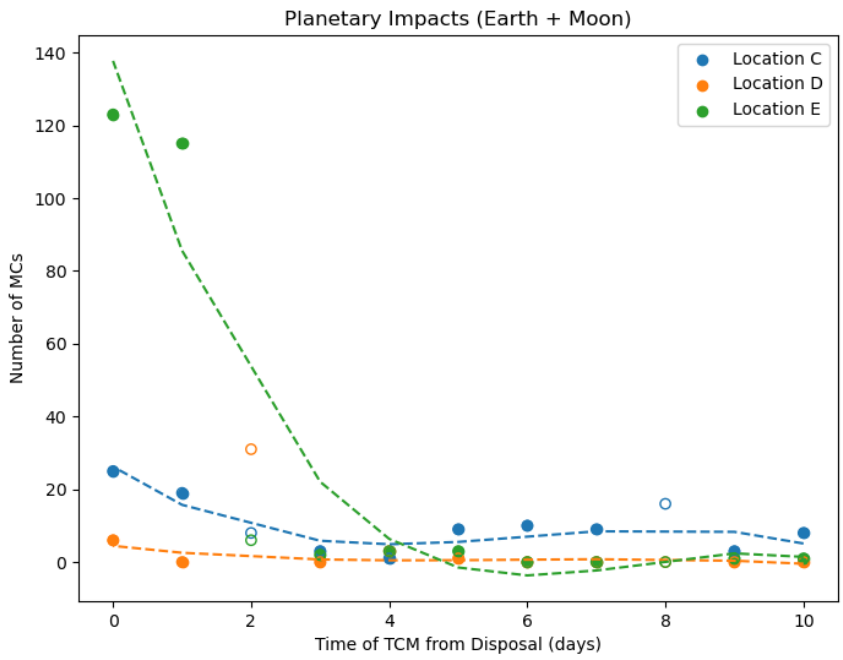

Figure 15: Number of monte carlo runs that impact either the Earth or the Moon

The intergrator was able to take much larger steps than it would for an Earth centered disposal propagation. Most Monte Carlo runs stayed close to the nominal of about 2000 steps. However, a couple of trajectories (one to three) in the two-day or later final TCMs reached steps higher than 5000. Most of the sets studied here do not have trajectories reaching that number of steps. The occurrences the integrator jumps up to this high of a step count is because the vehicle was likely caught by the Earth-Moon system and spent time there.

Usually when a vehicle is caught it either comes down to impact the Earth or is spit back out to a heliocentric orbit, which is why we don't see the increase in error for over ninety-nine percent of the trajectories. There lies a pretty large exception for location E where the no TCM or one-day TCM case had 155 and 175 trajectories respectively that reached over 5000 steps. These trajectories' badness are shown in the reach Earth's sphere of influence chart and thus are not necessarily singled out in this section. Although integrator performance is important for figuring out the exact propagation of a trajectory, the statistical nature of this analysis allows the authors to speak on the trends more broadly, and none of the Monte Carlo sets with small or little interactions with the Earth-Moon system also appeared to have substantial error growth through increased steps.

7 CONCLUSIONS

The three cases studied all showed sensitivity to time of contact for a heliocentric disposal sequence. The Sun-Earth-Moon geometry of the departure proved to greatly affect the dispersions for small times of contact. This is likely due to the shorter times in the Earth-Moon system having more energetic departures and thus less neighboring trajectories that have unfavorable paths. Interestingly, for longer times of contact with the disposal, the trends even out among the differ-

ent geometries and may prove to have diminishing returns as trajectory correction maneuvers are allowed to extend for longer times of flight.

Because there are so little trajectories that impact the Earth and Moon for final trajectory correction maneuvers greater than six days, it would probably be worth the effort to run a study with a much larger Monte Carlo set distribution. For the 1000 Monte Carlo runs done in this study, we see that adding in other forms of monitoring the trajectory behavior such as interactions below the Earth's Geosynchronous orbit helps provide additional context for how many Monte Carlo runs get close to impacting the Earth.

The placement of the trajectory correction maneuver is highly dependent on each nominal departure. While there are some well known truths shown in this data set, not placing a burn near perilune for one, there are other notable takeaways. For example, in this study five days was chosen as the placement for the first burn for the longer time of contact arcs. It might be more advantageous to conduct that first TCM burn earlier in the trajectory so that the trajectory isn't allowed to deviate as much from the nominal earlier in the process. This could be why there isn't as much performance payback in the later final burn results and the Earth interactions tend to level out around the eight day mark for most of the trajectories. There could also be additional constraints added to the targeter for solving the trajectory correction maneuvers. However, this is not straightforward as the larger amount of constraints on the problem the less likely the Monte Carlo case will solve.

If time of contact post mission is a limiting parameter on the disposal, vehicle operators can time the mission for the revolution on the NRHO that has the most ideal Sun-Earth-Moon geometry two times each revolution of the NRHO (one for exterior studied here and one idealized for interior). Even with large departure burns studied here, the geometry of NRHO perilunes and the L1 and L2 portals limit the effectiveness of guaranteeing a safe departures for short times of contact.

ACKNOWLEDGMENTS

The authors would like to thank Peter Brandt for developing the method of adding uncertainty in Monte Carlo modeling for Copernicus used in this paper.

REFERENCES

[1] S. Fuller, E. Lehnhardt, C. Zaid, and K. Halloran, "Gateway program status and overview," *Journal of Space Safety Engineering*, Vol. 9, No. 4, 2022, pp. 625–628.

[2] D. C. Davis, F. S. Khoury, K. C. Howell, and D. J. Sweeney, "Phase control and eclipse avoidance in near rectilinear halo orbits," *AAS guidance, navigation and control conference*, No. JSC-E-DAA-TN77422, 2020.

[3] G. L. Condon, C. A. Ocampo, L. Burke, C. C. Esty, C. Berry, B. Mahajan, and S. P. Downs, "Mission and trajectory design considerations for a human lunar mission originating from a near rectilinear halo orbit," *AIAA Scitech 2020 Forum*, 2020, p. 1921.

[4] G. Gargioni, D. Alexandre, M. Peterson, and K. Schroeder, "Multiple asteroid retrieval mission from lunar orbital platform-gateway using reusable spacecrafts," *40th IEEE Aerospace Conference*, 2019.

[5] D. J. Kessler, N. L. Johnson, J. Liou, and M. Matney, "The kessler syndrome: implications to future space operations," *Advances in the Astronautical Sciences*, Vol. 137, No. 8, 2010, p. 2010.

[6] H. Krag, S. Lemmens, T. Flohrer, and H. Klinkrad, "Global trends in achieving successful end-of-life disposal in LEO and GEO," *SpaceOps 2014 Conference*, 2014, p. 1933.

[7] M. Pellegrino, D. Scheeres, and B. Streetman, "Fragment Cloud Evolution in Medium Earth Orbit," *The Journal of the Astronautical Sciences*, Vol. 69, No. 6, 2022, pp. 1766–1796.

[8] A. Black and C. Frueh, "Fragmentation characterization in the circular restricted three body problem for cislunar space domain awareness," *Advances in Space Research*, Vol. 75, No. 1, 2025, pp. 1177–1204.

[9] N. R. Boone and R. A. Bettinger, "Debris collision risk analysis following simulated cislunar spacecraft explosions," *Journal of Spacecraft and Rockets*, Vol. 60, No. 2, 2023, pp. 668–684.

[10] P. Guardabasso, D. K. Skoulidou, L. Bucci, F. Letizia, S. Lemmens, M. Ansart, X. Roser, S. Lizy-Destrez, and G. Casalis, "Analysis of accidental spacecraft break-up events in cislunar space," *Advances in Space Research*, Vol. 72, No. 5, 2023, pp. 1550–1569.

[11] N. Boone, R. Bettinger, and B. Little, "Risks from Spacecraft Breakup Events in Near Rectilinear Halo Orbits," *Proceedings of the Advanced Maui Optical and Space Surveillance (AMOS) Technologies Conference*, 2023, p. 79.

[12] J. V. Breakwell and J. V. Brown, "The 'halo'family of 3-dimensional periodic orbits in the Earth-Moon restricted 3-body problem," *Celestial mechanics*, Vol. 20, No. 4, 1979, pp. 389–404.

[13] K. C. Howell, B. T. Barden, and M. W. Lo, "Application of dynamical systems theory to trajectory design for a libration point mission," *The Journal of the Astronautical Sciences*, Vol. 45, 1997, pp. 161–178.

[14] W. S. Koon, M. W. Lo, J. E. Marsden, and S. D. Ross, "Dynamical systems, the three-body problem and space mission design," *Equadiff 99: (In 2 Volumes)*, pp. 1167–1181, World Scientific, 2000.

[15] K. K. Boudad, D. C. Davis, and K. C. Howell, "Disposal trajectories from near rectilinear halo orbits," *AAS/AIAA Astrodynamics Specialists Conference*, No. JSC-E-DAA-TN60056, 2018.

[16] D. C. Davis, K. K. Boudad, S. M. Phillips, and K. C. Howell, "Disposal, deployment, and debris in near rectilinear halo orbits," *AAS/AIAA Space Flight Mechanics Meeting*, No. JSC-E-DAA-TN64520, 2019.

[17] D. C. Davis, K. K. Boudad, R. J. Power, K. C. Howell, and D. J. Sweeney, "Heliocentric escape and lunar impact from near rectilinear halo orbits," *AAS/AIAA Astrodynamics Specialists Conference*, No. JSC-E-DAA-TN72013, 2019.

[18] D. C. Davis, G. M. Brown, S. T. Scheuerle, E. M. Zimovan-Spreen, and K. C. Howell, "Jettisons from the Gateway Near Rectilinear Halo Orbit to Heliocentric Space: Applications and Practical Considerations," *AAS/AIAA Astrodynamics Specialist Conference*, No. AAS 24-326, 2024.

[19] S. T. Scheuerle, D. C. Davis, E. M. Zimovan-Spreen, B. P. McCarthy, D. B. Henry, and K. C. Howell, "Jettison and Disposal from Near Rectilinear Halo Orbits, Part 1: Theory," *American Astronautical Society Astrodynamics Specialists Conference*, No. AAS 23-311, 2023.

[20] D. C. Davis, S. T. Scheuerle, S. L. McCarty, E. M. Zimovan-Spreen, B. P. McCarthy, M. L. McGuire, and K. C. Howell, "Jettison and Disposal From Near Rectilinear Halo Orbits, Part 2: Applications," *AAS/AIAA Astrodynamics Specialist Conference*, No. AAS 23-306, 2023.

[21] J. Williams, J. S. Senent, C. Ocampo, R. Mathur, and E. C. Davis, "Overview and software architecture of the copernicus trajectory design and optimization system," *4th International Conference on Astrodynamics Tools and Techniques*, No. JSC-CN-20553, 2010.

[22] D. E. Lee, "White paper: Gateway destination orbit model: A continuous 15 year nrho reference trajectory," tech. rep., 2019.